Tantalum Hydrides Supported on MCM-41 Mesoporous Silica: Activation of Methane and Thermal Evolution of the Tantalum-Methyl Species

Sophie Soignier,[†] Mostafa Taoufik,[†] Erwan Le Roux,[†] Guillaume Saggio,[†] Céline Dablemont,[†] Anne Baudouin,[†] Frederic Lefebvre,[†] Aimery de Mallmann,[†] Jean Thivolle-Cazat,[†] Jean-Marie Basset,*[,†] Glenn Sunley,[‡] and Barry M. Maunders[§]

Laboratoire de Chimie Organométallique de Surface (UMR 9986 CNRS/ESCPE Lyon), ESCPE Lyon, F-308, 43 Boulevard du 11 Novembre 1918, F-69616 Villeurbanne Cedex, France, BP Chemicals Ltd, Hull Research and Technology Center, Saltend, Hull, HU128DS, U.K., and BP Chemicals Ltd, Chertsey Road Sunbury On Thames, Middlesex, TW16 7LL, U.K.

Received July 21, 2005

The Ta(=CH*t*Bu)(CH_2*t*Bu)$_3$ complex **1** reacts with the OH groups of a MCM-41 mesoporous silica dehydroxylated at 500 °C to form the monosiloxy surface species [(≡SiO)Ta(=CH*t*Bu)(CH_2*t*Bu)$_2$] **2**, with evolution of 1 equiv per Ta of neopentane. Complex **2** leads to a mixture of supported tantalum hydrides [(≡SiO)$_2$Ta(H)$_x$] (x = 1, 3), **3**, by treatment under hydrogen at 150 °C. These surface complexes were characterized by the combined use of several techniques such as IR and EXAFS spectroscopies as well as ^{1}H MAS, ^{13}C CP/MAS, 2D ^{1}H−^{13}C HETCOR, and *J*-resolved solid-state NMR and mass balance analysis. The surface tantalum hydrides evolve reversibly to the monohydride species (≡SiO)$_2$Ta-H by heating at 150 °C under vacuum; they lead progressively to the complete formation of the supported trisiloxy tantalum complex (≡SiO)$_3$Ta by heating under hydrogen (600 Torr) up to 500 °C. They can activate at 150 °C the C−H bond of CH_4 to form first the surface tantalum methyl species [(≡SiO)$_2$Ta-(CH_3)$_x$] with liberation of H_2. The initially rapid decrease of the ν(Ta−H) bands followed by a slower rate indicates the presence of a distribution of Ta-H sites of various reactivity. The combined use of ^{13}C CP/MAS solid-state NMR and 100% ^{13}C-labeled methane affords the observation of methylidene and methylidyne species on a few tantalum sites, which indicates the occurrence of an α-H elimination process. In parallel, a progressive transfer of methyl groups from tantalum to neighboring siloxane bridges was also evidenced, which grows with temperature; this process is reasonably accompanied by the formation of the trisiloxy tantalum complex (≡SiO)$_3$Ta.

Introduction

The transformation of light paraffins is always of great interest in the field of academic and industrial research, especially for petrochemical applications. Notably the transformation of methane is an important challenge, due to its abundance on earth, but also to its chemical inertia.[1−4] Activation of the C−H and C−C bonds of alkanes has been the subject of numerous studies involving early and late transition metals as well as lanthanide or actinide molecular complexes.[5−7] The interaction of organometallic complexes with the surface of oxides such as silica or alumina has been studied for about four decades.[8−11] The applications of the resulting materials were mainly oriented to the catalysis of various chemical reactions, particularly polymerization but also hydrogenation, olefin metathesis, and oxidation. In this field, alkyl−alkylidene tantalum complexes grafted on silica (≡SiO)Ta(=CH*t*Bu)(CH_2*t*Bu)$_2$ and (≡SiO)$_2$Ta-(=CH*t*Bu)(CH_2*t*Bu)[12−15] were prepared, which led to supported tantalum hydride (≡SiO)$_2$TaH[16] by treatment under hydrogen at 150 °C. This latter complex is able to activate the C−H bond of methane and cycloalkanes[16,17] and catalyze the H/D exchange reaction with alkanes[18] or the hydrogenolysis[19,20] and the

* To whom correspondence should be addressed. E-mail: basset@cpe.fr.
† Laboratoire de Chimie Organométallique de Surface.
‡ BP Chemicals Ltd, Hull.
§ BP Chemicals Ltd, Middlesex.

(1) Mimoun, H. *New J. Chem.* **1987**, *11*, 513−525.
(2) Crabtree, R. H. *Chem. Rev.* **1995**, *95*, 987−1007.
(3) Shilov, A. E.; Shul'pin, G. B. *Chem. Rev.* **1997**, *97*, 2879−2932.
(4) Crabtree, R. H. *J. Chem. Soc., Dalton Trans.* **2001**, 2437−2450.
(5) Crabtree, R. H. *Chem. Rev.* **1985**, *85*, 245−269.
(6) Hill, C. L. *Activation and Functionalisation of Alkanes*; Wiley: New York, 1989.
(7) Bhasin, M. M.; Slocum, D. W. *Methane and Alkane Conversion Chemistry*; Plenum Press: New York, 1995.
(8) Ballard, D. G. H. *Adv. Catal.* **1973**, *23*, 263−325.
(9) Yermakov, Y. I.; Kuznetsov, B. N.; Zakharov, V. A. *Stud. Surf. Sci. Catal.* **1981**, *8*, 1.
(10) Basset, J. M.; Choplin, A. *J. Mol. Catal.* **1983**, *21*, 95−108.
(11) Scott, S. L.; Basset, J. M.; Niccolai, G. P.; Santini, C. C.; Candy, J. P.; Lecuyer, C.; Quignard, F.; Choplin, A. *New J. Chem.* **1994**, *18*, 115−122.
(12) Dufaud, V.; Niccolai, G. P.; Thivolle-Cazat, J.; Basset, J.-M. *J. Am. Chem. Soc.* **1995**, *117*, 4288−4294.
(13) Lefort, L.; Chabanas, M.; Maury, O.; Meunier, D.; Copéret, C.; Thivolle-Cazat, J.; Basset, J.-M. *J. Organomet. Chem.* **2000**, *593*−*594*, 96−100.
(14) Chabanas, M.; Quadrelli, E. A.; Fenet, B.; Copéret, C.; Thivolle-Cazat, J.; Basset, J.-M.; Lesage, A.; Emsley, L. *Angew. Chem., Int. Ed.* **2001**, *40*, 4493−4496.
(15) Le Roux, E. L.; Chabanas, M.; Baudouin, A.; de Mallmann, A.; Copéret, C.; Quadrelli, E. A.; Thivolle-Cazat, J.; Basset, J.-M.; Lukens, W.; Lesage, A.; Emsley, L.; Sunley, G. J. *J. Am. Chem. Soc.* **2004**, *126*, 13391−13399.
(16) Vidal, V.; Theolier, A.; Thivolle-Cazat, J.; Basset, J.-M.; Corker, J. *J. Am. Chem. Soc.* **1996**, *118*, 4595−4602.
(17) Vidal, V.; Theolier, A.; Thivolle-Cazat, J.; Basset, J.-M. *J. Chem. Soc., Chem. Commun.* **1995**, 991−992.
(18) Lefort, L.; Copéret, C.; Taoufik, M.; Thivolle-Cazat, J.; Basset, J.-M. *Chem. Commun.* **2000**, 663−664.

10.1021/om050609e CCC: $33.50
Publication on Web 02/23/2006

metathesis of alkanes.[21,22] The tantalum species as well as various surface organometallic complexes developed in the same way[23] were characterized by a panel of physical and chemical methods, according to the surface organometallic chemistry (SOMC) approach, which is aimed at the transfer of concepts and tools from molecular chemistry to surface science.[24] Recently, the development of advanced spectroscopic techniques has enabled the improvement of the characterization to determine the ligand arrangement in the coordination sphere of the grafted metal.[14,25−27]

This paper deals with the interaction of the [Ta(=CH*t*Bu)-(CH_2*t*Bu)$_3$] complex with the surface of a MCM-41 mesoporous silica partially dehydroxylated at 500 °C, which by its high surface area affords high tantalum loading; this factor combined with the use of a ^{13}C-enriched tantalum complex leads to an improved characterization of the resulting surface tantalum species. The transformation under hydrogen of the resulting surface alkyl−alkylidene tantalum complex into the supported hydride has been studied as well as the thermal stability of the latter. Finally, the reactivity of this surface tantalum hydride with methane and the thermal evolution of the tantalum methyl species have been considered and discussed as an illustration of elementary steps that can take place during surface reactions involving alkanes.

Results and Discussions

Grafting of [Ta(=CH*t*Bu)(CH_2*t*Bu)$_3$], 1, on MCM-41$_{(500)}$. In Situ IR Study. When an excess of [Ta(=CH*t*Bu)(CH_2*t*Bu)$_3$], **1**, is sublimed at 80 °C on a MCM-41 mesoporous silica disk (1060 m^2/g, 28 Å pore size) partially dehydroxylated at 500 °C (namely, MCM-41$_{(500)}$), the disk turns immediately yellow, and the ν(O−H) band at 3747 cm^{-1} assigned to the isolated silanol groups disappears according to IR spectroscopy. A broad band of weak intensity appears at lower wavenumbers (3740−3550 cm^{-1}), showing the presence of a small amount of residual silanols. Concomitantly, two groups of bands appear in the 3000−2700 and 1500−1300 cm^{-1} regions, assigned to ν(C−H) and δ(C−H) vibrations of the perhydrocarbyl ligands reasonably bonded to tantalum, and neopentane is released in the gas phase. These ν(C−H) and δ(C−H) bands resist desorption, which supports the occurrence of an irreversible grafting reaction of **1** onto the MCM-41 surface. As already reported with flame silica (Aerosil degussa 200m^2/g),[12−15] the consumption of silanol groups and the release of neopentane indicate the substitution of some neopentyl ligands on **1**, by surface siloxy groups, leading to complex **2**.

Mass Balance Analyses. To establish the mass balance of this grafting reaction, it was carried out on a larger scale with MCM-41 powder, by sublimation or impregnation with a pentane solution of **1**. Again, the solid progressively turned yellow and neopentane evolved in the gas phase. However, whereas on Aerosil silica treated at the same temperature i.e., 500 °C, a mixture of mono- and bibonded species [(≡SiO)Ta-(=CH*t*Bu)(CH_2*t*Bu)$_2$] and [(≡SiO)$_2$Ta(=CH*t*Bu)(CH_2*t*Bu)] was obtained,[12,13] the following characterizations indicate that on MCM-41 only the monografted species is formed (Scheme 1): (i) whatever the preparation method used (sublimation or impregnation of powder in pentane solution) only 1 equiv of neopentane per grafted tantalum is evolved; (ii) the elemental analysis of the solid after elimination of all physisorbed species fits with the formula of a monografted complex (a 15.5 C/Ta ratio was found with 13.8 wt % C and 13.4 wt % Ta, whereas a theoretical ratio of 15 is expected for the monografted complex and of 10 for the bigrafted complex with three or two neopentyl-like remaining ligands, respectively); (iii) the treatment at 150 °C under H_2 of the grafted complex affords the liberation of 14.9 methane molecules per grafted tantalum, which is consistent with the previous data. All these data are therefore consistent with the formation of a monobonded surface complex as the major species, which according to the valence 5 of tantalum can be formulated as [(≡SiO)Ta(=CH*t*Bu)(CH_2*t*Bu)$_2$], **2**. The difference in behavior concerning the nature of supported species between nonporous flame silica and mesoporous MCM-41 was already observed in the case of zirconium organometallic complexes.[28] It is also worth mentioning that the use of a support of higher surface area affords a tantalum loading twice to three times higher than on flame silica (13.4 instead of 5−6 wt %). However, the average surface density of Ta appears lower on MCM-41 than on silica, whereas surface OH densities are comparable (~1.4 ± 0.1 OH/nm^2); in fact the consumption of OH groups proves lower on MCM-41, probably because steric effects inside the pores can limit the access of the tantalum complex either to some OH groups (for example in the corners of hexagonal pores) or even to some pores themselves (pore blockage).

Scheme 1. Reactivity of [Ta(=CH*t*Bu)(CH_2*t*Bu)$_3$], 1, with MCM-41$_{(500)}$: Formation of [≡SiO−Ta(=CH*t*Bu)(CH_2*t*Bu)$_2$], 2

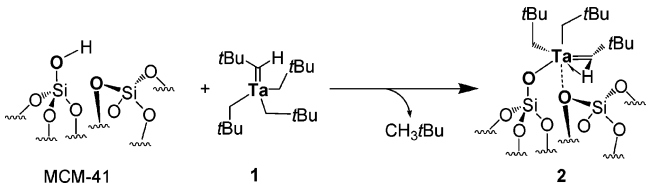

Solid-State NMR Spectroscopy and EXAFS. The ^{1}H solid-state MAS NMR spectrum of **2** displays two signals at 1.0 and 4.3 ppm (see Figure S1a in the Supporting Information), while the ^{13}C solid-state CP/MAS NMR spectrum shows four signals at 33.4, 45.7, 95, and 247 ppm, which can be assigned to C(*C*H$_3$)$_3$, *C*(CH$_3$)$_3$, (*C*H$_2$*t*Bu), and (=*C*H*t*Bu) resonances, respectively (Figure S1b). The higher loading of Ta (13.4%) obtained after grafting **1** on MCM-41 affords a ^{13}C NMR spectrum of better quality compared to Aerosil silica, [12] in particular with the presence of the small peak at 247 ppm. To still improve the signal-to-noise ratio,[29−32] the ^{13}C-enriched

(19) Chabanas, M.; Vidal, V.; Copéret, C.; Thivolle-Cazat, J.; Basset, J.-M. *Angew. Chem., Int. Ed.* **2000**, *39*, 1962−1965.
(20) Rataboul, F.; Chabanas, M.; De Mallmann, A.; Copéret, C.; Thivolle-Cazat, J.; Basset, J.-M. *Eur. J. Chem.* **2003**, *9*, 1426−1434.
(21) Vidal, V.; Theolier, A.; Thivolle-Cazat, J.; Basset, J.-M. *Science* **1997**, *276*, 99−102.
(22) Maury, O.; Lefort, L.; Vidal, V.; Thivolle-Cazat, J.; Basset, J.-M. *Angew. Chem., Int. Ed.* **1999**, *38*, 1952−1955.
(23) Lefebvre, F.; Thivolle-Cazat, J.; Dufaud, V.; Niccolai, G. P.; Basset, J.-M. *Appl. Catal. A* **1999**, *182*, 1−8.
(24) Copéret, C.; Chabanas, M.; Petroff Saint-Arroman, R.; Basset, J.-M. *Angew. Chem., Int. Ed.* **2003**, *42*, 156−181.
(25) Petroff Saint-Arroman, R.; Chabanas, M.; Baudouin, A.; Copéret, C.; Basset, J.-M.; Lesage, A.; Emsley, L. *J. Am. Chem. Soc.* **2001**, *123*, 3820−3821.
(26) Lesage, A.; Emsley, L.; Chabanas, M.; Copéret, C.; Basset, J.-M. *Angew. Chem., Int. Ed.* **2002**, *41*, 4535−4538.
(27) Chabanas, M.; Baudouin, A.; Copéret, C.; Basset, J.-M.; Lukens, W.; Lesage, A.; Hediger, S.; Emsley, L. *J. Am. Chem. Soc.* **2003**, *125*, 492−504.
(28) Wang, X.-X.; Veyre, L.; Lefebvre, F.; Patarin, J.; Basset, J.-M. *Microporous Mesoporous Mater.* **2003**, *66*, 169−179.
(29) Jezequel, M.; Dufaud, V.; Ruiz-Garcia, M. J.; Carrillo-Hermosilla, F.; Neugebauer, U.; Niccolai, G. P.; Lefebvre, F.; Bayard, F.; Corker, J.; Fiddy, S.; Evans, J.; Broyer, J.-P.; Malinge, J.; Basset, J.-M. *J. Am. Chem. Soc.* **2001**, *123*, 3520−3540.
(30) Toscano, P. J.; Marks, T. J. *Organometallics* **1986**, *5*, 400−402.

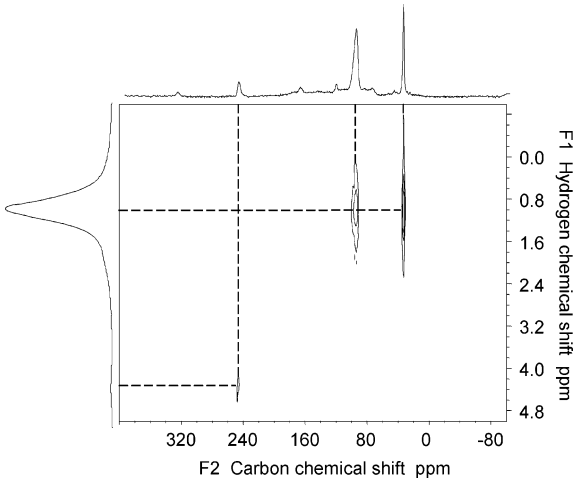

Figure 1. $^{1}H-^{13}C$ HETCOR solid-state NMR spectrum of **2*** (NS 4168, D1 = 1 s, P15 = 2 ms, LB = 80 Hz).

complex **1***, 10% randomly labeled on the α-position, was prepared and grafted on MCM-41$_{(500)}$. While the ^{1}H NMR spectrum of the resulting surface complex **2*** is quite similar to that of **2**, its ^{13}C CP/MAS NMR spectrum now shows an increased signal at 247 ppm (Figure S2) correlated to the signal at 4.3 ppm in the ^{1}H dimension, by 2D $^{1}H-^{13}C$ HETCOR NMR (Figure 1), consistent with the presence of a neopentylidene ligand; moreover, a higher intensity is obtained for the signal at 95 ppm correlated to the proton at 1.0 ppm, corresponding to the methylene group of neopentyl ligands (Figure 1). Additionally, the 2D spectrum shows the usual correlation between the signals at 33.4 and 1.0 ppm, but no correlation for the ^{13}C signal at 47.5 ppm, consistent with their assignments to methyl groups and quaternary carbons, respectively; these observations were already made previously in the case of nonporous silica.[14] Again, as observed with Aerosil silica,[15] or the molecular silsesquioxane analogue,[14] the low $^{1}J_{C-H}$ value for the α-carbenic proton (80 Hz) detected by *J*-resolved 2D solid-state NMR (Figure S3) might indicate a weak agostic interaction of this proton with the metal center.[33−38]

EXAFS studies performed on [(≡SiO)Ta(=CHCMe$_3$)(CH$_2$-CMe$_3$)$_2$], **2** (Figure 2 and Table 1), give a first shell of two neighbors (one oxygen and one carbon atom: −*O*Si≡ and =*C*H*t*Bu, not resolved), at 1.914 Å, then two other carbons at 2.13 Å (*C*H$_2$*t*Bu) and a second shell composed of an extra oxygen atom at 2.99 Å (≡Si−*O*−Si≡) and three carbon atoms at 3.42 Å (=CH*C*Me$_3$ or CH$_2$*C*Me$_3$). Again, the higher tantalum loading on MCM-41 affords an improved treatment of the EXAFS spectrum on a wider range of *k* values (2.4 to 16 instead of 2 to 13 Å^{-1} previously[15]). However, the EXAFS results are quite similar to those obtained on flame silica SiO$_{2-(700)}$[15] and in addition to NMR, confirm the structure previously proposed for complex **2** (Scheme 1), where the presence of a two-electron donor siloxane bridge (≡Si−O−Si≡) and the agostic neopentylidene proton affords the stabilization of a highly electron deficient complex (formally a 12-electron species).

Reactivity of the Grafted [(≡SiO)Ta(=CH*t*Bu)(CH$_2$*t*Bu)$_2$] Complex with Hydrogen: Formation of Tantalum Hydrides. When [(≡SiO)Ta(=CH*t*Bu)(CH$_2$*t*Bu)$_2$] supported on MCM-41$_{(500)}$, **2**, is heated at 150 °C under hydrogen, the pale yellow solid darkens to brown and leads to solid **3**. Methane is evolved (14.9 CH$_4$ per grafted tantalum), resulting from the hydrogenolysis of much of the hydrocarbyl ligands in **2**. IR spectroscopy shows the formation of both silicon and tantalum hydrides (ν(Si−H) at 2210 and 2280 cm^{-1} and ν(Ta−H) at 1838 cm^{-1}), in agreement with previous studies performed with Aerosil silica.[13,16] However, since the metal loading is ca. 3 times higher on MCM-41 than on Aerosil silica, the detection of some minor species is improved. For example, in the ^{1}H MAS solid-state NMR spectrum (Figure S4), besides two intense peaks at 1.8 and 0.8 ppm, respectively assigned to residual silanols and alkyl fragments, additional weak signals appear in the 20−30 ppm range, which could be assigned to some Ta-H hydride species (probably tantalum(V) trishydrides that are present as minor species (vide infra)) (Scheme 2); the ^{1}H NMR signal at 4.2 ppm can be readily assigned to Si-H species,[39] which is consistent with the bands at 2210 and 2280 cm^{-1} observed in the IR spectrum.[40,41] Interestingly, the ^{29}Si CP/MAS NMR spectrum of [(≡SiO)Ta(=CH*t*Bu)(CH$_2$*t*Bu)$_2$] before reaction with hydrogen shows only a broad signal around −101 ppm, due to residual silanol groups (≡SiO)$_3$*Si*(OH) (Q^3) with their nearest neighbors (≡SiO)$_4$*Si* (Q^4) and (≡SiO)$_2$*Si*(OH)$_2$ (Q^2) at −109 and − 91 ppm, respectively (Figure 3a)[42−44] Note that this spectrum is quite comparable to that of silica dehydroxylated at high temperature. After reaction with hydrogen, the spectrum is more interesting, as it shows an additional peak at ca. −78 ppm assigned to (≡*Si*−H) or (=*Si*−H$_2$) fragments, in agreement with IR spectroscopy, which are usually believed to form by opening of neighboring siloxane bridges and transfer of hydrogen atoms on the surface (Figure 3b and Scheme 2). This peak value is consistent with the reported literature data for T^3 sites.[42−44]

EXAFS studies performed on tantalum hydride **3** (Figure 4, Table 2) show a first shell of about two oxygen atoms at 1.91 Å (≡Si−*O*) and, at longer distances, the contribution of other oxygen atoms at 2.65 and 2.91 Å (≡Si−*O*−Si≡) or silicon atoms at 3.32 and 3.56 Å ((≡SiO)$_3$*Si*−O). During calculations, the possible presence of tantalum clusters or particles was also considered. However, the good fit obtained on a wide *k* range, from 2.4 to 16.3 Å^{-1}, was not improved by considering a Ta−Ta contribution. It led to a very small Ta−Ta distance (less than 2.7 Å), incompatible with literature data on multinuclear tantalum species; a high Debye−Waller factor ($\sigma > 0.11$ Å) was also obtained for this contribution, with very few Ta neighbors ($N_{Ta} < 0.5$). We can then conclude that most of the tantalum hydrides are present as mononuclear species in this sample. These results are comparable to those obtained on flame

(31) Finch, W. C.; Gillespie, R. D.; Hedden, D.; Marks, T. J. *J. Am. Chem. Soc.* **1990**, *112*, 6221−6232.
(32) Ahn, H.; Marks, T. J. *J. Am. Chem. Soc.* **2002**, *124*, 7103−7110.
(33) Schrock, R. R. *Acc. Chem. Res.* **1979**, *12*, 98−104.
(34) Brookhart, M.; Green, M. L. H. *J. Organomet. Chem.* **1983**, *250*, 395−408.
(35) Nugent, W. A.; Mayer, J. M. *Metal−Ligand Multiple Bond*; Wiley: New York, 1988.
(36) Schultz, A. J.; Williams, J. M.; Schrock, R. R.; Rupprecht, G. A.; Fellmann, J. D. *J. Am. Chem.* Soc. **1979**, *101*, 1593−1595.
(37) Goddard, R. J.; Hoffmann, R.; Jemmis, E. D. *J. Am. Chem. Soc.* **1980**, *102*, 7667−7676.
(38) Fellmann, J. D.; Schrock, R. R.; Traficante, D. D. *Organometallics* **1982**, *1*, 481−484.
(39) Campbell-Ferguson, H. J.; Ebsworth, E. A. V.; MacDiarmid, A. G.; Yoshioka, T. *J. Phys. Chem.* **1967**, *71*, 723−726.
(40) Quignard, F.; Lecuyer, C.; Bougault, C.; Lefebvre, F.; Choplin, A.; Olivier, D.; Basset, J. M. *Inorg. Chem.* **1992**, *31*, 928−930.
(41) Quignard, F.; Lecuyer, C.; Choplin, A.; Olivier, D.; Basset, J. M. *J. Mol. Catal.* **1992**, *74*, 353−363.
(42) Bourgeat-Lami, E.; Lefebvre, F. *Macromolecules* **2002**, *35*, 6185−6191.
(43) Corriu, R. J. P.; Mehdi, A.; Reye, C.; Thieuleux, C.; Frenkel, A.; Gibaud, A. *New J. Chem.* **2004**, *28*, 156−160.
(44) Corriu, R. J. P.; Mehdi, A.; Reye, C.; Thieuleux, C. *Chem. Mater.* **2004**, *16*, 159−166.

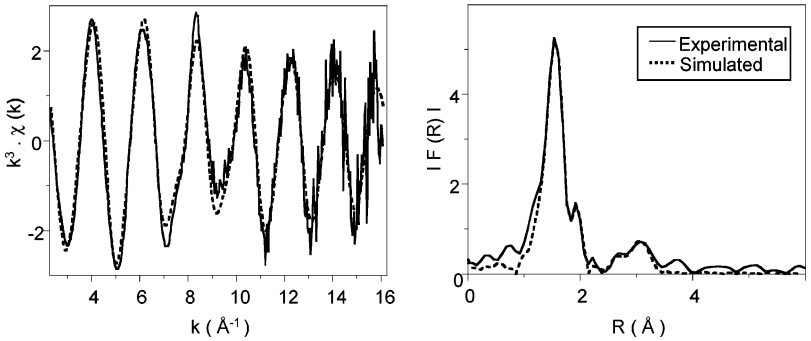

Figure 2. Ta L_{III}-edge k^3-weighted EXAFS (left) and Fourier transform (right) of **2**. Solid lines: experimental; dashed lines: spherical wave theory.

Scheme 2. Supported [(≡SiO)$_2$Ta(H)$_x$] Species, 3, along with the (≡Si−H) Fragment upon Treatment of [≡SiO−Ta(=CH*t*Bu)(CH$_2$*t*Bu)$_2$], 2, under H$_2$ at 150 °C

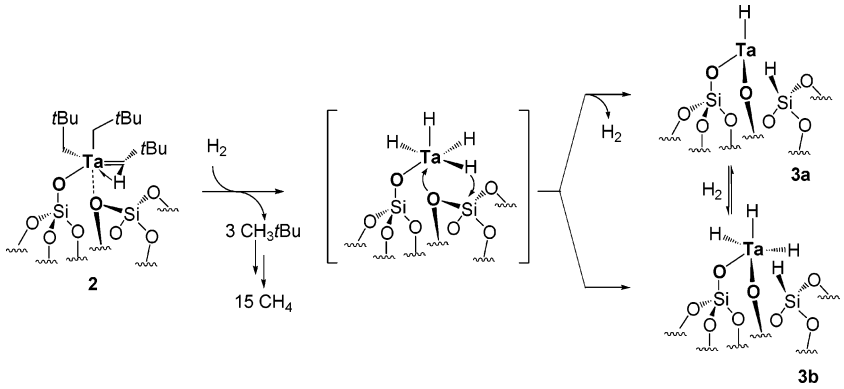

Table 1. EXAFS Parameters for [(≡SiO)Ta(=CH*t*Bu)(CH$_2$*t*Bu)$_2$(≡SiOSi≡)], 2[a]

neighboring atom of Ta	no. of atoms	distance (Å)	Debye−Waller factor (σ/Å)
−*O*Si	1.2	1.914(8)	0.04(2)
=*C*HCMe$_3$	1.0	1.914[b]	0.05(2)
−*C*H$_2$CMe$_3$	2.0	2.13(2)	0.08(3)
*O*Si$_2$	1.0	2.99(5)	0.09(5)
CH$_x$*C*Me$_3$	3.0	3.42(3)	0.08(4)

[a] Fit residue: $\rho = 9\%$ ($\Delta k = 2.4-16$ Å^{-1}); same energy shift for all shells: $\Delta E_0 = 5.1(9)$ eV; overall scale factor: $S_0^2 = 1.0$. [b] Shell constrained to the parameter above.

silica SiO$_{2(500)}$[16] and confirm the structure previously proposed for complex **3** (Scheme 2), with the presence of one or two electron donor siloxane bridges (≡Si−O−Si≡) in the neighborhood of the metal; this may afford the stabilization of a highly electron deficient complex (formally an 8- to 12-electron species).

Thermal Stability of the Tantalum Hydrides, 3, under Hydrogen and under Vacuum. The tantalum hydride supported on silica (≡SiO)$_2$Ta-H is known to evolve by heating under hydrogen to 500 °C, to the naked trisiloxy tantalum complex (≡SiO)$_3$Ta by opening of the surrounding siloxane bridges and transfer of hydrogen onto the surface silicon atoms.[45] The same behavior was checked by IR spectroscopy with the tantalum hydride supported on MCM-41 mesoporous silica; a sample of **3** was progressively heated under H_2, to 500 °C, by increments of 50 °C, for periods of 2 h. The corresponding IR spectra show the continuous and progressive decrease of the ν(Ta−H) vibration bands and the concomitant growth of the ν(Si−H) bands (Figure S5), suggesting that a hydrogen transfer still takes place between the tantalum center and neighboring silicon atoms, leading to the same trisiloxy tantalum complex (≡SiO)$_3$Ta, **4** (Scheme 3).

To complete the study of the thermal stability, the tantalum hydride, **3**, was heated at 150 °C under vacuum. A rapid 40% decrease of the ν(Ta−H) bands was observed before reaching a plateau after about 5 h (Figure S6a). Reloading with hydrogen (650 Torr) and heating at 150 °C regenerated the initial ν(Ta−H) bands; this result strongly suggests the existence, for some

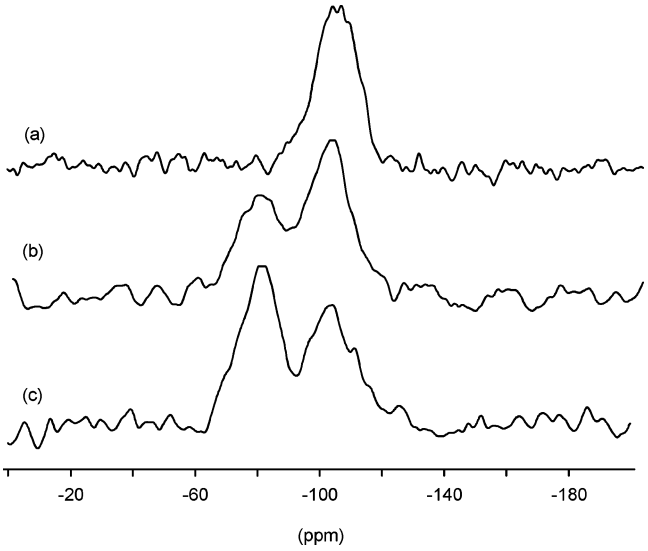

Figure 3. ^{29}Si solid-state CP/MAS NMR spectra (a) of solid **2** obtained after grafting of molecular complex **1** on MCM-41$_{(500)}$; (b) after treatment of solid **2**, under H_2 at 150 °C for 15 h: solid **3**; (c) after treatment of solid **3**, under CH_4 at 250 °C for 26 h. (NS 50000, D1 = 1 s, P15 = 1 ms, LB = 80 Hz.)

(45) Saggio, G.; de Mallmann, A.; Maunders, B.; Taoufik, M.; Thivolle-Cazat, J.; Basset, J.-M. *Organometallics* **2002**, *21*, 5167−5171.

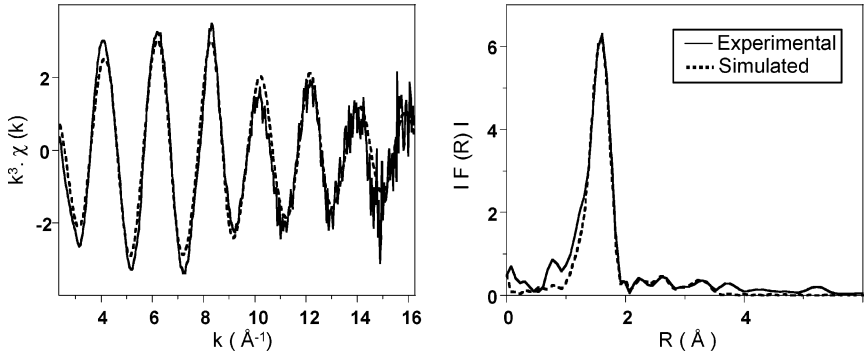

Figure 4. Ta L_{III}-edge k^3-weighted EXAFS (left) and Fourier transform (right) of **3**. Solid lines: experimental; dashed lines: spherical wave theory.

Table 2. EXAFS Parameters for [(≡SiO)$_2$Ta(H)$_x$], 3[a]

neighboring atom of Ta	no. of atoms	distance (Å)	Debye−Waller factor (σ/Å)
−*O*Si	2.4(4)	1.910(5)	0.053(5)
*O*Si$_2$	0.5(7)	2.65(6)	0.07(6)
*O*Si$_2$	0.6(9)	2.91(7)	0.07[b]
−O*Si*	1.0(6)	3.32(9)	0.10(7)
−O*Si*	1.0[b]	3.56(8)	0.10[b]

[a] Fit residue: $\rho = 8\%$ ($\Delta k = 2.4-16.3$ Å^{-1}); same energy shift for all shells: $\Delta E_0 = 6.4(9)$ eV; overall scale factor: $S_0^2 = 1.0$. [b] Shell constrained to the parameter above.

Scheme 3. Supported [(≡SiO)$_3$Ta] Species along with the (≡Si−H) Fragment upon Treatment of [(≡SiO)$_2$Ta(H)$_x$], 3a and 3b, under H_2 to 500 °C

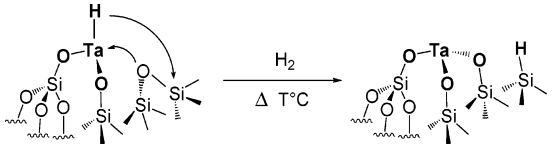

tantalum sites, of an equilibrium between mono- and trishydrido forms since the usual oxidation states of tantalum are 3 and 5 (Scheme 2).

Reactivity of the Tantalum Hydrides, 3, with Methane. In Situ IR Study. Silica-supported tantalum hydride is known to activate the C−H bond of methane or cycloalkanes to form the corresponding surface tantalum alkyl species with liberation of 1 equiv of hydrogen.[16,17,46] It is also a catalyst precursor for the alkane metathesis reaction[21,22] that transforms an alkane into its higher and lower homologues and is believed to involve carbene and tantallacyclobutane intermediates similar to those of olefin metathesis.[15,47−49] Although complex **2** already bears a carbene ligand and is also a catalyst precursor for the alkane metathesis when grafted on silica,[50] it was interesting to investigate more thoroughly the activation of methane by the tantalum hydrides, **3**, to check the possible evolutions of the expected tantalum methyl species without the risk of a β-H elimination process.[51−58] Methane activation was then monitored by IR spectroscopy versus time and took place significantly only after heating at 150 °C; a rapid decrease of the ν(Ta−H) band was initially observed, followed by a slower decreasing rate; no change could be evidenced in the ν(C−H) region, as the expected methyl ligand usually gives too tiny signals. After 20 h, 60% of the ν(Ta−H) band had disappeared, whereas 0.94 equiv of H_2 per Ta was liberated in the gas phase. The hydrolysis of the solid obtained afforded the liberation of 0.6 equiv of CH_4 per Ta. The excess of hydrogen relative to the ν(Ta−H) band consumption reasonably confirms the presence of 20−30% of a tantalum trishydrido form. In a second experiment, the tantalum hydride, **3**, was then heated at 150 °C under vacuum to convert the trishydrido into the monohydrido form. A 40% decrease of the ν(Ta−H) band was again observed before stabilization after 5 h. Methane was introduced and activated again at 150 °C. The remaining ν(Ta−H) bands followed again a rapid then a slower decrease of a total of 55% after 20 h (Figure S7). After evacuation and reloading with methane, only the slow activation process was taking place, leading to a 10% more ν(Ta−H) band decrease, in 20 h. The total consumption of ν(Ta−H) bands was only achieved after heating at 250 °C for 20 h more. This experiment thus indicates a heterogeneity of the tantalum hydride sites regarding the CH bond activation of methane as it was already observed in the case of cycloalkanes.[46] Highly reactive sites react first and involve the rapid ν(Ta−H) band decrease followed by the slow reaction of less reactive sites. Moreover, the absence of effect of the methane reloading on the CH bond activation rate suggests that this reaction is not limited by an eventual equilibrium.

Solid-State NMR Spectroscopy. To check the evolution of surface tantalum methyl species versus time and temperature as well as the possible effect of the heterogeneity of the tantalum sites, a study by ^{13}C CP MAS NMR using ^{13}C-labeled methane was performed. After reaction of $^{13}CH_4$ with the solid **3** at 150 °C for 24 h, the ^{13}C CP MAS NMR spectrum shows three broad peaks centered at 57, 200, and 330 ppm (Figure 5a). These peaks have chemical shifts compatible with methyl (51 and 62 ppm), methylidene (200 ppm), and methylidyne (330 ppm) ligands, respectively. Several carbene complexes of Ta are known,[59−63] and for example, in the case of $Cp_2Ta(=CH_2)CH_3$ the carbons

(46) Maury, O.; Saggio, G.; Theolier, A.; Taoufik, M.; Vidal, V.; Thivolle-Cazat, J.; Basset, J.-M. *C. R. Acad. Sci*. **2000**, *3*, 583−587.
(47) Herisson, J. L.; Chauvin, Y. *Makromol. Chem.* **1971**, *141*, 161−176.
(48) Ivin, K. J.; Mol, I. C. *Olefin Metathesis and Metathesis Polymerization*, 2nd ed.; Academic Press: New York, 1996.
(49) Basset, J.; Copéret, C.; Lefort, L.; Maunders, B.; Maury, O.; Le Roux, E.; Saggio, G.; Soignier, S.; Soulivong, D.; Sunley, G.; Taoufik, M.; Thivolle-Cazat, J. *J. Am. Chem. Soc.* **2005**, *127*, 8604−8605.
(50) Copéret, C.; Maury, O.; Thivolle-Cazat, J.; Basset, J.-M. *Angew. Chem., Int. Ed.* **2001**, *40*, 2331−2334.
(51) Watson, P. L.; Roe, D. C. *J. Am. Chem. Soc.* **1982**, *104*, 6471−6473.
(52) Watson, P. L.; Parshall, G. W. *Acc. Chem. Res.* **1985**, *18*, 51−56.
(53) Parkin, G.; Bunel, E.; Burger, B. J.; Trimmer, M. S.; Van Asselt, A.; Bercaw, J. E. *J. Mol. Catal.* **1987**, *41*, 21−39.
(54) Bunel, E.; Burger, B. J.; Bercaw, J. E. *J. Am. Chem. Soc.* **1988**, *110*, 976−978.
(55) Schock, L. E.; Marks, T. J. *J. Am. Chem. Soc.* **1988**, *110*, 7701−7715.
(56) Buchwald, S. L.; Nielsen, R. B. *Chem. Rev.* **1988**, *88*, 1047−1058.
(57) Burger, B. J.; Thompson, M. E.; Cotter, W. D.; Bercaw, J. E. *J. Am. Chem. Soc.* **1990**, *112*, 1566−1577.
(58) Negishi, E.-I.; Takahashi, T. *Acc. Chem. Res.* **1994**, *27*, 124−130.
(59) Messerle, L. W.; Jennische, P.; Schrock, R. R.; Stucky, G. *J. Am. Chem. Soc.* **1980**, *102*, 6744−6752.

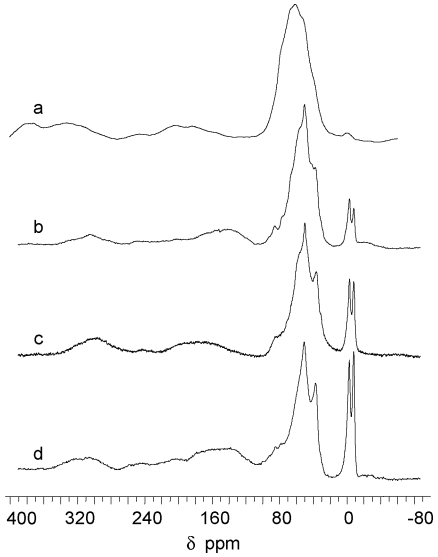

Figure 5. Study by ^{13}C CP/MAS solid-state NMR of the $^{13}CH_4$ activation on $[(\equiv SiO)_2Ta(H)_x]$, **3**, (a) at 150 °C during 24 h or (b) at 250 °C for 3 h; (c) then for 23 h; (d) then under argon for 43 h.

of the methyl and the methylidene have chemical shifts at 57 and 224 ppm, respectively.[64] Carbyne complexes of Ta are less common, but examples exist and present chemical shifts between 300 and 350 ppm.[65,66] These observations indicate that the methyl species formed after activation of CH_4 on **3**, at 150 °C, can undergo a partial evolution to a mixture of unsaturated surface species such as $[(\equiv SiO)_2Ta(=CH_2)(H)]$ and $[(\equiv SiO)_2Ta\equiv CH]$ probably by the involvement of successive α-H elimination processes (Scheme 4).[53,59,64,67−71] Increasing the number of bonds between tantalum and carbon results in an increase of the line width due to a higher effect of the surface heterogeneity and of the different surroundings of tantalum.

$^{13}CH_4$ activation was also performed at 250 °C, showing in this case by ^{13}C CP/MAS NMR better defined peaks of carbene and carbyne species at 180 and 296 ppm, respectively (Figure 5b,c). The tantalum methyl species shifted to a peak centered at 50 ppm with a shoulder at 36 ppm. In addition, new signals appear at −3 and −8 ppm, which can reasonably be attributed to (≡Si−Me) or (=Si(H)Me) species. Interestingly, the corresponding ^{29}Si CP/MAS NMR spectrum shows an increase of the peak at −78 ppm initially assigned to (≡Si−H) or ($=SiH_2$) species and which would also fit with Si-methyl ones (Figure 3b,c). The peaks at −3 and −8 ppm in the ^{13}C NMR increase progressively, under methane or argon atmospheres (Figure 5c,d), by prolonged heating at 250 °C and even more accurately at 300 °C (Figure S8). The presence of such surface methylsilane species suggests by analogy with the appearance of (≡Si-H) groups during the formation of the tantalum hydride, **3**, the occurrence of a methyl transfer from the Ta center to a surface Si atom by opening of a neighboring siloxane bridge and concomitant formation of $[(\equiv SiO)_3Ta]$ (Scheme 5).[45] 2D $^1H-^{13}C$ HETCOR solid-state NMR (Figure 6) confirms the attribution of the (Si-Me) and (Ta-Me) in the ^{13}C MAS NMR; two correlations are observed between the signals at 0.2 and 0.3 ppm in the ^1H dimension, which are attributed to the methyl groups linked to a surface silicon atom, and the signals at −3 and −8 ppm in the ^{13}C dimension. Moreover, two ^1H resonances of methyl groups at 0.9 and 1.5 ppm correlate with carbons at 50 and 36 ppm, respectively, showing a heterogeneous environment of the Ta-methyl species. However, no correlation could be detected for the carbene and carbyne signals, which are too tiny.

The heterogeneity of surface tantalum sites revealed by the kinetics of CH bond activation of methane and the various evolution of tantalum methyl species can be correlated to a possible structure formulation in agreement with EXAFS results. In the case of the surface tantalum hydride, **3**, as well as the alkyl−alkylidene complex, **2**, the refinement of the simulated EXAFS spectra implies the participation of some surface oxygen atoms in a second shell, which would stabilize these highly electron deficient tantalum species. Since in the former case, the stoichiometries of these oxygen atoms relative to tantalum are not whole numbers, this could be due to the heterogeneity of the tantalum environment. More precisely, tantalum sites that are close to the oxygen of a siloxane bridge may be hindered to activate methane and further to undergo α-H elimination but conversely would progressively transfer to the surface, the methyl linked to tantalum (Scheme 5). Tantalum sites that are not so close to surface oxygen could correspond to the trishydride; they would activate methane more easily, but the resulting tantalum-methyl could then evolve to carbene or carbyne species since α-H elimination would not be hindered (Scheme 4). The latter could also be involved as active sites in the alkane metathesis reaction since carbene species are believed to be intermediates[15,49] and turn out to be formed after the activation of an alkane. To support this proposition, it was observed that the presence of trimethylphosphine coordinated to the tantalum hydride[72] totally inhibited the activity for alkane metathesis as do surface oxygen too close to the metal. For this reaction also, the formation of a carbyne complex could be a dead end or at least a less active species.

Conclusion

We have shown that the $Ta(=CH\mathit{t}Bu)(CH_2\mathit{t}Bu)_2$ complex (**1**) reacts with the OH groups of a MCM-41 mesoporous silica dehydroxylated at 500 °C to form the monosiloxy surface species $[(\equiv SiO)Ta(=CH\mathit{t}Bu)(CH_2\mathit{t}Bu)_2]$ (**2**), with evolution of 1 equiv per Ta of neopentane. Complex **2** leads to a mixture of supported tantalum hydrides $[(\equiv SiO)_2Ta(H)_x]$ ($x = 1, 3$), **3**, by treatment under hydrogen at 150 °C. These surface complexes were characterized by the combined use of several techniques such as IR and EXAFS spectroscopies as well as ^1H MAS, ^{13}C CP/MAS, 2D $^1H-^{13}C$ HETCOR, and *J*-resolved solid-state NMR and mass balance analysis. The surface tantalum hydrides, **3**, evolve reversibly to the monohydride species $(\equiv SiO)_2Ta$-H

(60) Schultz, A. J.; Brown, R. K.; Williams, J. M.; Schrock, R. R. *J. Am. Chem. Soc.* **1981**, *103*, 169−176.
(61) Schrock, R. R. *ACS Symp. Ser.* **1983**, *211*, 369−382.
(62) Schrock, R. R. *Reactions of Coordinated Ligands*; Braterman Paul, S., Ed.; Plenum Press: New York, 1986; Vol. 1.
(63) Berry, D. H.; Koloski, T. S.; Carroll, P. J. *Organometallics* **1990**, *9*, 2952−2962.
(64) Van Asselt, A.; Burger, B. J.; Gibson, V. C.; Bercaw, J. E. *J. Am. Chem. Soc.* **1986**, *108*, 5347−5349.
(65) Churchill, M. R.; Wasserman, H. J.; Turner, H. W.; Schrock, R. R. *J. Am. Chem. Soc.* **1982**, *104*, 1710−1716.
(66) Fellmann, J. D.; Turner, H. W.; Schrock, R. R. *J. Am. Chem. Soc.* **1980**, *102*, 6608−6609.
(67) Schrock, R. R.; Fellmann, J. D. *J. Am. Chem. Soc.* **1978**, *100*, 3359−3370.
(68) Sharp, P. R.; Schrock, R. R. *J. Organomet. Chem.* **1979**, *171*, 43−51.
(69) Schrock, R. R.; Shih, K.-Y.; Dobbs, D. A.; Davis, W. M. *J. Am. Chem. Soc.* **1995**, *117*, 6609−6610.
(70) Schrock, R. R. *Acc. Chem. Res.* **1997**, *30*, 9−16.
(71) Hierso, J.-C.; Etienne, M. *Eur. J. Inorg. Chem.* **2000**, 839−842.
(72) Taoufik, M.; de Mallmann, A.; Prouzet, E.; Saggio, G.; Thivolle-Cazat, J.; Basset, J.-M. *Organometallics* **2001**, *20*, 5518−5521.

Scheme 4. Reaction Pathway Leading to $[(\equiv SiO)_2Ta-CH_3]$, by Activation of CH_4 on $[(\equiv SiO)_2Ta(H)_x]$, 3, Then to $[(\equiv SiO)_2Ta(=CH_2)(H)]$ and $[(\equiv SiO)_2Ta(\equiv CH)]$, by Successive α-H Elimination

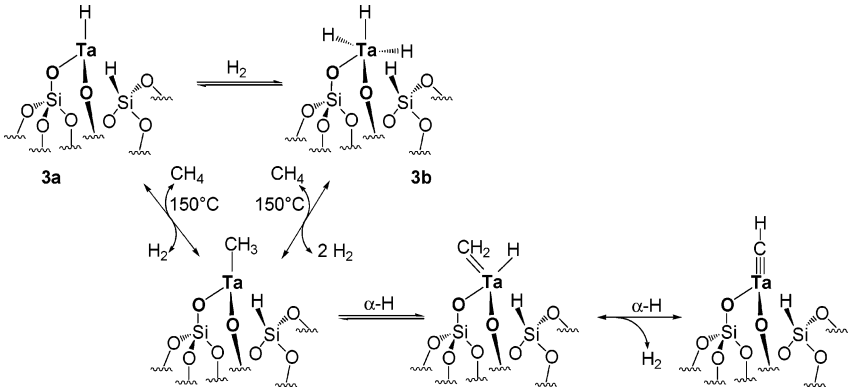

Scheme 5. Formation of $[(\equiv SiO)_3Ta]$ Species along with the $(\equiv Si-Me)$ Fragment upon Treatment of $[(\equiv SiO)_2Ta(H)_x]$, 3a and 3b, under CH_4 at 250−300 °C

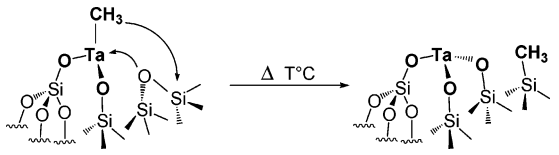

by heating at 150 °C under vacuum; they lead progressively to the complete formation of the supported trisiloxy tantalum complex $(\equiv SiO)_3Ta$ by heating under hydrogen (600 Torr) up to 500 °C. They can activate at 150 °C the C−H bond of CH_4 to form first surface tantalum methyl species $[(\equiv SiO)_2Ta(CH_3)_x]$ with liberation of H_2. The initially rapid decrease of the ν(Ta−H) bands followed by a slower rate indicates the presence of a distribution of Ta-H sites of various reactivity. The combined use of ^{13}C CP/MAS solid-state NMR and 100% ^{13}C-labeled methane afforded the observation of methylidene and methylidyne species, which indicates the occurrence of α-H elimination processes on a few tantalum sites not hindered by the proximity of siloxane bridges. In parallel, a progressive transfer of methyl groups from tantalum to neighboring siloxane bridges was also evidenced, which grows with temperature; this process is reasonably accompanied by the formation of the trisiloxy tantalum complex $(\equiv SiO)_3Ta$ just like during thermal treatment under hydrogen.

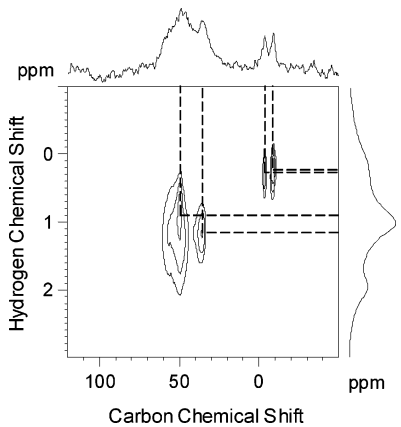

Figure 6. $^1H-^{13}C$ 2D HETCOR solid-state NMR spectrum of $^{13}CH_4$ activated at 250 °C for 26 h on the solid $[(\equiv SiO)_2Ta(H)_x]$, **3** (NS = 3072, D1 = 2 s, P15 = 5 ms, LB^1H = 100 Hz, $LB^{13}C$ = 100 Hz).

Experimental Section

General Procedure. All experiments were carried out under controlled atmosphere, using Schlenk and glovebox techniques for the organometallic synthesis. For the synthesis and treatments of the surface species, reactions were carried out using high-vacuum lines (1.34 Pa) and glovebox techniques. $[Ta(=CHtBu)(CH_2tBu)_3]$ and the corresponding ^{13}C-enriched complexes were prepared by the reaction of $TaCl_5$ with $tBuCH_2MgCl$ according to the literature procedure.[67] $tBuCH_2MgCl$ was prepared from $tBuCH_2Cl$ (98%, Aldrich, used as received) and Mg turnings (Lancaster). $[Ta(=^{13}CHtBu)(^{13}CH_2tBu)_2]$, **1***, 10% randomly enriched on the α-position, was prepared starting from ^{13}C-labeled (carbonyl ^{13}C, 99%) dimethylformamide (DMF*) and using the following reaction sequence: reaction of *t*BuLi with DMF* to form (^{13}C, 99%)-2,2-dimethylpropanal, followed by a reduction with $LiAlH_4$ to yield the corresponding alcohol. Nucleophilic substitution with the Vilsmeier reagent $[ClCH=N(CH_3)_2]Cl$[73,74] gave 2,2-dimethylchloropropane, 99% ^{13}C enriched on the α-position. It was then transformed into the corresponding Grignard reagent. After dilution with unlabeled neopentylmagnesium chloride, the reaction with $TaCl_5$ gave **1***, in which the carbons directly bonded to Ta were randomly ^{13}C-enriched to the extent of 10%. The molecular complex **1*** was finally grafted on $MCM\text{-}41_{(500)}$ to yield **2***.

Pentane and diethyl ether were distilled on NaK alloy and Na/benzophenone, respectively, followed by degassing through freeze−pump−thaw cycles.

Infrared spectra were recorded on a Nicolet Magna 550 FT spectrometer equipped with a cell fitted with CaF_2 windows and designed for in situ reactions under controlled atmosphere.

Elemental analyses were performed at the Service Central d'Analyses of CNRS in Solaize.

^1H MAS and ^{13}C CP-MAS solid-state NMR spectra were recorded on a Bruker DSX-300 spectrometer. For specific studies (see below), ^1H MAS and ^{13}C CP-MAS solid-state NMR spectra were recorded on a Bruker Avance-500 spectrometer with a conventional double resonance 4 mm CP-MAS probe at the Laboratoire de Chimie Organométallique de Surface in Ecole Supérieure de Chimie Physique Electronique de Lyon. The samples were introduced under Ar in a zirconia rotor, which was then tightly closed. In all experiments, the rotation frequency was set to 10 kHz unless otherwise specified. Chemical shifts were given with respect to TMS as external references for ^1H and ^{13}C NMR.

Heteronuclear Correlation Spectroscopy. The two-dimensional heteronuclear correlation experiment was performed according to the following scheme: 90° proton pulse, t_1 evolution period, cross-

(73) Cheon, J.; Rogers, D. M.; Girolami, G. S. *J. Am. Chem. Soc.* **1997**, *119*, 6804−6813.

(74) Bruno, J. W.; Smith, G. M.; Marks, T. J.; Fair, C. K.; Schultz, A. J.; Williams, J. M. *J. Am. Chem. Soc.* **1986**, *108*, 40−56.

polarization (CP) to carbon spins, detection of carbon magnetization. For the CP step, a ramp radio frequency (rf) field[75,76] centered at 60 kHz was applied on protons, while the carbon rf field was matched to obtain optimal signal. The contact time for CP was set to 1 ms. During acquisition, the proton decoupling field strength was set to 83 kHz (TPPM decoupling[77]). A total of 32 t_1 increments with 1024 scans each were collected. The spinning frequency was 10 kHz, and the recycle delay was 1 s (total acquisition time of 9 h). Quadrature detection in ω_1 was achieved using the TPPI method.[78]

***J*-Resolved Spectroscopy.** The two-dimensional *J*-resolved experiment was performed as previously described:[26] after cross-polarization from protons, carbon magnetization evolves during t_1 under proton homonuclear decoupling. Simultaneous 180° carbon and proton pulses are applied in the middle of t_1 to refocus the carbon chemical shift evolution while retaining the modulation by the heteronuclear J_{CH} scalar couplings. A Z-filter is finally applied to allow phase-sensitive detection in ω_1. Proton homonuclear decoupling was performed by using the frequency-switched Lee-Goldburg (FSLG) decoupling sequence.[79,80] Quadrature detection in ω_1 was achieved using the TPPI method.[78] The rotor spinning frequency was 10.2 kHz in order to synchronize the t_1 increment with the rotor period. The proton rf field strength was set to 83 kHz during t_1 (FSLG decoupling) and acquisition (TPPM decoupling).[77] The lengths of carbon and proton 180° pulses were 7 and 6 μs, respectively. An experimental scaling factor, measured as already described,[81] of 0.52 was found, which gave a corrected spectral width of 2452 Hz in the ω_1 dimension. The recycle delay was 1.3 s, and a total of 80 t_1 increments with 1024 scans each were collected (total acquisition time = 30 h).

Extended X-ray Absorption Fine Structure Spectroscopy (EXAFS). The samples **2** and **3** were packaged within an argon-filled drybox in double airtight sample holders equipped with Kapton windows. X-ray absorption spectra were acquired at the Laboratoire pour l'Utilisation du Rayonnement Electromagnétique (LURE), on the DCI ring at beam line D44. They were recorded at room temperature at the tantalum L_{III} edge, from 9700 to 11 000 eV, with a 2 eV step in the transmission mode. The data analyses were performed by standard procedures using the suite of programs developed by A. Michalowicz.[82] Each spectrum was carefully extracted, and the best removal of low-frequency noise was checked by further Fourier transformation. Fitting of the spectrum was done on the k^3-weighted data using the following EXAFS equation where S_0^2 is the scale factor; N_i is the coordination number of shell i; S_i is the central atom loss factor for atom i; F_i is the EXAFS scattering function for atom i; R_i is the distance to atom i from the absorbing atom; λ_i is the photoelectron mean free path; σ_i is the Debye−Waller factor; ϕ_i is the EXAFS phase function for atom i; and ϕ_c is the EXAFS phase function for the absorbing atom.

$$\chi(k) = S_0^2 \sum_{i=1}^{n} \frac{N_i S_i(k, R_i)\, F_i(k, R_i)}{kR_i^2} \exp\left(\frac{-2R_i}{\lambda(k, R_i)}\right) \times \exp(-2\sigma_i^2 k^2) \sin[2kR_i + \phi_i(k, R_i) + \phi_c(k)]$$

The program FEFF7[83] was used to calculate theoretical values for S_i, F_i, λ_i, ϕ_i, and ϕ_c based on model clusters of atoms in which atomic positions were taken from the crystal structure of the most similar complexes. The refinements were performed by fitting the structural parameters N_i, R_i, and σ_i and the energy shift, ΔE_0 (the same for all shells). The fit residue, ρ, was calculated by the following formula:

$$\rho = \frac{\sum_k [k^3\chi_{exp}(k) - k^3\chi_{Cal}(k)]^2}{\sum_k [k^3\chi_{exp}(k)]^2}$$

Preparation of MCM-41$_{(500)}$. The MCM-41 mesoporous silica was supplied by the Laboratoire des Matériaux Minéraux, E. N. S. de Chimie de Mulhouse, 3 Rue Alfred Werner, 68093 Mulhouse Cédex, France. It was prepared according to a literature method.[84] Its BET surface area, determined by nitrogen adsorption at 77 K, is 1060 m^2/g with a mean pore diameter of 28 Å (BJH method). The wall thickness was found to be 14 Å by subtraction of the pore diameter from the unit cell parameter deduced from X-ray powder diffraction data.

Preparation of 2 and 3 in an IR Cell. Complex **1** was sublimed on a self-supporting pellet (17 mm diameter; 12 mg) of MCM-41 previously treated at 500 °C under vacuum for 15 h, in the IR cell (280 mL). The pellet immediately turns yellow, neopentane is evolved in the gas phase, and the excess of unreacted complex is desorbed by back-sublimation at 80 °C. The formation of **2** is thus monitored by IR spectroscopy (CaF_2 windows). After evacuation of the gas phase, hydrogen (600Torr) is introduced and the cell is heated at 150 °C for 15 h, leading to the formation of complex **3** and the liberation of light alkanes.

Preparation of Solid 2 by Impregnation in Pentane. In a two-sided reaction vessel equipped with a fritted glass, a solution of **1** (516 mg, 1.11 mmol) in dried pentane (15 mL) was added (through the frit) to the MCM-41$_{(500)}$ powder (1 g, 2.1 to 3.5 mmol OH/g) recovered with pentane. The solid becomes yellow, and after 2 h of stirring at room temperature the material turns pale orange. After filtration of the floating solution, the solid was washed four times with pentane and all volatile compounds were condensed into another reactor of known volume, to quantify neopentane evolved during the grafting. The resulting pale orange powder was dried under vacuum (10^{-5} Torr) to yield 1.33 g of **2**.

Preparation of Solid 2* by Impregnation in Pentane. The ^{13}C-enriched surface compound **2*** was prepared according to the same procedure as described above by using **1*** in place of **1**.

Treatment under H_2 of Solid 2 (quantification of neopentyl-like ligands and formation of solid 3). In a 500 mL glass reactor, 70 mg of **2** (13.88 wt %, 0.054 mmol of Ta) was introduced under argon. After evacuation of the gas phase, hydrogen (600 Torr, 320 equiv/Ta) was added. The mixture was heated at 150 °C and sampled to follow by GC analysis the evolution of light alkanes resulting from the hydrogenolysis of neopentyl-like ligands.

Thermal Stability of Solid 3 under H_2. After formation of solid **3**, the IR cell was evacuated and refilled with hydrogen (600 Torr); the IR pellet (12 mg) supporting **3** was progressively heated to 500 °C in increments of 50 °C for 2 h, leading to the formation of **4**; the evolution of surface species was monitored by IR spectroscopy.

Thermal Stability of Solid 3 under Vacuum. After formation of solid **3**, the IR cell was evacuated. The IR pellet (12 mg) supporting **3** was heated at 150 °C under dynamic vacuum. After

(75) Hediger, S.; Meier, B. H.; Kurur, N. D.; Bodenhausen, G.; Ernst, R. R. *Chem. Phys. Lett.* **1994**, *223*, 283−288.
(76) Metz, G.; Wu, X.; Smith, S. O. *J. Magn. Reson. A* **1994**, *110*, 219−227.
(77) Bennett, A. E.; Rienstra, C. M.; Auger, M.; Lakshmi, K. V.; Griffin, R. G. *J. Chem. Phys.* **1995**, *103*, 6951−6958.
(78) Marion, D.; Wuethrich, K. *Biochem. Biophys. Res. Commun.* **1983**, *113*, 967−974.
(79) Bielecki, A.; Kolbert, A. C.; Levitt, M. H. *Chem. Phys. Lett.* **1989**, *155*, 341−346.
(80) Levitt, M. H.; Kolbert, A. C.; Bielecki, A.; Ruben, D. J. *Solid Stat. Nucl. Magn. Reson.* **1993**, *2*, 151−163.
(81) Lesage, A.; Duma, L.; Sakellariou, D.; Emsley, L. *J. Am. Chem. Soc.* **2001**, *123*, 5747−5752.
(82) Michalowicz, A. *Logiciels pour la Chimie*; Société Française de Chimie: Paris, 1991.
(83) Zabinsky, S. I.; Rehr, J. J.; Ankudinov, A.; Albers, R. C.; Eller, M. J. *Phys. Rev. B: Condens. Matter* **1995**, *52*, 2995−3009.
(84) Wang, X. X.; Patarin, F.; Lefebvre, F.; Basset, J. M. *Microporous Mesoporous Mater.* **2001**, *42*, 269.

refilling with hydrogen (600 Torr) the IR pellet was heated again at 150 °C to regenerate solid **3**, and the evolution of surface species was monitored by IR spectroscopy.

C−H Bond Activation of CH_4 on Solid 3 in the IR Cell. In the 280 mL infrared cell where complex **3** (13 mg; 15,8 wt % Ta) was prepared under hydrogen, methane was introduced (660 Torr, 980 equiv/Ta) after evacuation of the gas phase; the cell was heated at 150 °C, and the reaction was monitored by IR spectroscopy (decrease of ν(Ta−H) bands) and GC (evolution of hydrogen).

Activation of $^{13}CH_4$ on Solid 3. Similarly, complex **3** (88 mg, 13.37 wt % Ta, 0.065 mmol) prepared in the 500 mL batch reactor was allowed to react with $^{13}CH_4$ (660 Torr, 270 equiv/Ta) at 150 °C or/and 250 °C for 20 h in order to prepare samples for solid-state NMR.

Acknowledgment. We thank Dr. C. Copéret for helpful discussions. This work was sponsored by BP Chemicals, the CNRS, and ESCPE Lyon.

Supporting Information Available: ^{1}H MAS and ^{13}C CP/MAS solid-state NMR spectra of solids **2** and **2***, 2D *J*-resolved NMR spectrum of solid **2***, ^{1}H MAS NMR spectrum of solid **3**, IR spectra of the stability of solid **3** [$(\equiv SiO)_2Ta-H_x$] under vacuum or hydrogen, and ^{13}C CP/MAS NMR spectra of the evolution of Ta-methyl species at 300 °C. This material is available free of charge via the Internet at http://pubs.acs.org.

OM050609E